6-1998

fMRI of Monkey Visual Cortex

Lisa Stefanacci
University of California, La Jolla

Paul Reber
University of California, La Jolla

Jennifer Costanza
Salk Institute for Biological Studies

Eric Wong
University of California, La Jolla

Richard Buxton
University of California, San Diego

See next page for additional authors

Recommended Citation

Stefanacci, L., Reber, P., Costanza, J., Wong, E., Buxton, R., Zola, S., ... & Albright, T. (1998). fMRI of monkey visual cortex. Neuron, 20(6), 1051-1057. https://doi.org/10.1016/S0896-6273(00)80485-7

Authors
Lisa Stefanacci, Paul Reber, Jennifer Costanza, Eric Wong, Richard Buxton, Stuart Zola, Larry R. Squire, and Thomas D. Albright

Neuron, Vol. 20, 1051–1057, June, 1998, Copyright ©1998 by Cell Press

fMRI of Monkey Visual Cortex

Neurotechnique

Lisa Stefanacci,*#† Paul Reber,* Jennifer Costanza,† Eric Wong,*‡ Richard Buxton,‡ Stuart Zola,*§‖ Larry Squire,*§‖ and Thomas Albright†
*Department of Psychiatry
University of California
La Jolla, California 92093
†Howard Hughes Medical Institute
Salk Institute for Biological Studies
La Jolla, California 92037
‡Department of Radiology
University of California
San Diego, California 92103
§Department of Neurosciences
University of California
La Jolla, California 92093
‖Veterans Administration Medical Center
San Diego, California 92161

Summary

While functional magnetic resonance imaging (fMRI) is now used widely for demonstrating neural activity-related signals associated with perceptual, motor, and cognitive processes in humans, to date this technique has not been developed for use with nonhuman primates. fMRI in monkeys offers a potentially valuable experimental approach for investigating brain function, which will complement and aid existing techniques such as electrophysiology and the behavioral analysis of the effects of brain lesions. There are, however, a number of significant technical challenges involved in using fMRI with monkeys. Here, we describe the procedures by which we have overcome these challenges to carry out successful fMRI experiments in an alert monkey, and we present the first evidence of activity-related fMRI signals from monkey cerebral cortex.

Introduction

Functional magnetic resonance imaging (fMRI) is a promising new tool that has been used widely for localizing activity-dependent signals in the human brain during sensory, motor, and cognitive tasks (Belliveau et al., 1991; Courtney and Ungerleider, 1997; Raichle, 1998). The fMRI signal, which reflects changes in local cerebral blood flow and oxygenation, provides a noninvasive way to identify neural activity-related signals in the brain with better spatial resolution than other neuroimaging techniques, such as positron emission tomography (PET).

Despite the aggressive development of fMRI to identify functionally specialized regions in the human brain, this technique has not been heretofore successfully applied to nonhuman primates. Nonetheless, the successful use of fMRI in monkeys is of great potential value for rapidly identifying brain regions involved in perception, cognition, and motor function and as a complement to traditional experimental approaches such as single-cell electrophysiology, neuroanatomical tract tracing, and studies of the behavioral effects of focal brain lesions. Moreover, in combination with microelectrode recording, the application of fMRI in monkeys holds promise for clarifying the relationship between neuronal activity and the BOLD (blood oxygenation level–dependent) signal of fMRI.

There are a number of significant technical challenges involved in carrying out fMRI experiments in monkeys, arising from the need to use alert (unanesthetized) monkeys for the experiment. While apparatus and procedures for behavioral control of alert monkeys, and for their immobilization in a confined space, have been well developed for single-cell electrophysiological experiments and can be adapted for use in fMRI, there are some novel components that must be introduced to satisfy the constraints of the magnet environment. Primary among these is the fact that the alert animal must be restrained in a horizontal position to accommodate the bore of the magnet (unlike electrophysiolgical experiments, which are generally performed with the animal sitting erect and oriented vertically). The animal must also be trained to perform behavioral tasks in an extremely noisy and potentially distracting environment (owing to the mechanics of the MRI system) and in a highly confined space. In addition, the apparatus for restraining the monkey must be made from nonferrous materials that do not interfere in any way with fMRI signal acquisition.

Here, we describe the procedures by which we have successfully overcome these technical hurdles in order to carry out an fMRI experiment in an alert monkey. Additionally, we present the first evidence of activity-dependent fMRI signals from the cerebral cortex of an alert monkey.

Results

Subject

The subject was an adult female rhesus monkey (*Macaca mulatta*) weighing ~7.8 kg. The protocols used have been approved by the Salk Institute Animal Care and Use Committee and they conform to USDA regulations and NIH guidelines for the humane care and use of laboratory animals.

Apparatus

Primate Chairs

We designed two primate chairs to comfortably restrain the alert monkey. One chair was used during Phase 1 of the training session, and the other chair was used during Phase 2 of training and for the scanning sessions. The chair that we used during Phase 1 of the training procedure was modified from the standard primate restraint chair manufactured by Crist Instruments (Damascus, MD). The principal modification was designed to

To whom correspondence should be addressed at the Salk Institute.

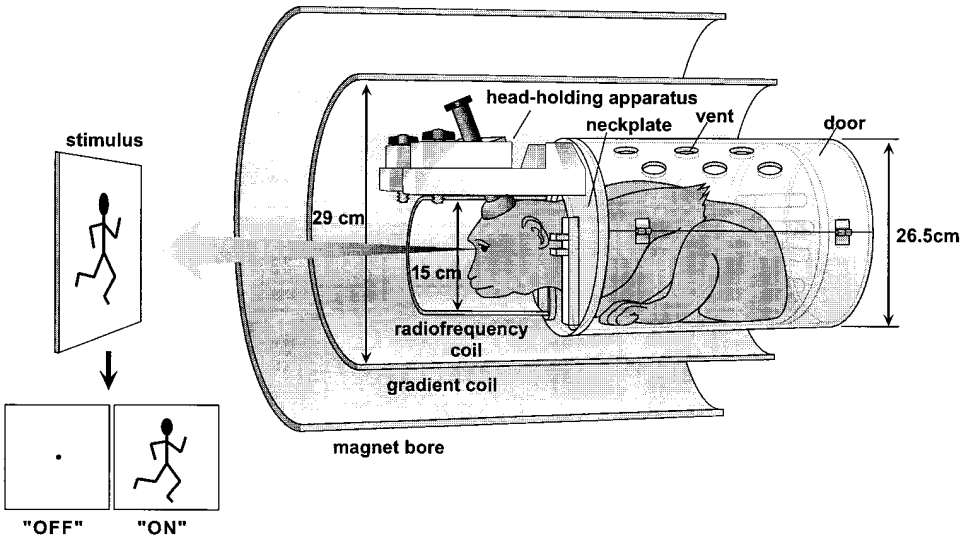

Figure 1. Set-up for Monkey fMRI
See text for details.

allow the chair to tilt forward. The chair could thus hold the monkey at any of five angles: 0°, 25°, 45°, 70°, and 90° (0° being vertical, the "standard" orientation, and 90° being horizontal/prone). Using a method of successive approximations, the monkey was tilted in this chair until she adapted to the prone position required to accommodate the horizontal bore of the magnet.

Size and material composition were two major constraints in designing a primate chair for Phase 2 of the training procedure and for the fMRI scanning session itself. Regarding size, the center of the monkey's head was to be inserted to a depth of 20 cm into a three-axis local head gradient coil that was cylindrically shaped and 29 cm in diameter (Wong et al., 1992a, Proc. Soc. Magn. Reson. Med., abstract; Figure 1). The upper portion of the primate chair was thus limited by this dimension and was designed to meet these constraints. The chair itself was fashioned from a 26.5 cm (outside diameter) acrylic cylinder. With respect to materials to be used during the fMRI scanning session, we limited ourselves to plastic parts (e.g., nylon screws) to avoid any possible distortion of the magnetic field.

Head-Holding Apparatus

In order to prevent motion artifact and to allow for more precise signal localization, we produced a nonmetallic apparatus to hold the monkey's head in a fixed position during Phase 2 of the training procedure and during the fMRI scanning sessions (Figure 2). A headframe and crossbar were built onto the neckplate of the primate chair. The crossbar supported the headbar, which attached to the cranial headpost that was surgically implanted onto the monkey's skull. When the monkey's head was in the fixed position, her head was oriented such that her line of sight was parallel to the long axis of the chair, which in turn was parallel to the horizontal bore of the magnet (Figure 1). Size and material composition were also limiting factors for the design of this head-holding apparatus. All points on the apparatus were contained within the 26.5 cm diameter cross-sectional profile of the restraint chair (Figure 1). The headframe and crossbar were constructed of acrylic and Delrin, with nylon screws. The headbar, surgically implanted cranial headpost, and cranial screws were fabricated from Cilux plastic by Crist Instruments (Damascus, MD).

Radiofrequency (RF) Coil

A radiofrequency (RF) coil (15 cm in diameter) was secured around the cranium by attachment to the chair. The coil was a scaled-down version of the birdcage coil originally described by Wong and colleagues for human

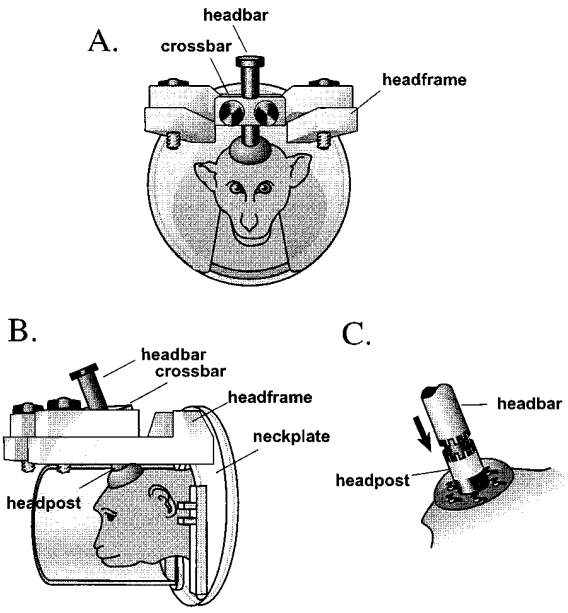

Figure 2. Monkey Head-Holding Apparatus
See text for details.

fMRI (1992b, Proc. Soc. Magn. Reson. Med., abstract) and was built upon a Plexiglas cylinder infrastructure. A small slit (10 cm × 2 cm) was cut into the plastic of the RF coil so that the headpost could be lowered through and attached to the monkey's head.

Mock fMRI Environment

In order to habituate the monkey to confinement and audible noise, the monkey was preconditioned for the scanning sessions in an apparatus that simulated the MR environment (Figure 1). The apparatus included "mock" gradient and RF coils, a simulated magnet bore, and a tape that played recorded pulse sequences from an actual fMRI scanning session at sound intensity levels that gradually, over ∼20 daily sessions (5 sessions/week), came to approximate those of the MR environment.

Visual Stimulus and Visual Stimulation Device

A major goal of these experiments was to demonstrate activity-dependent signals in the visual cortex of a monkey during the passive viewing of a visual stimulus. In order to observe a large signal, we selected a visual stimulus that was dynamic and rich in color, contrast, and texture, i.e., a children's animated movie (Gymboree, Warner Brothers), reproduced in standard VHS video format. The stimulus was rear-projected onto a screen that was positioned at the end of the magnet bore, ∼1.75 m from the nodal point of the monkey's eye. The visible portion of the screen was limited by the circular bore of the magnet and, on the lower margin, by the patient platform, which extended out from the bore to the screen. As a result, the stimulus appeared within a ∼25° diameter circular aperture, excluding the segment defined by a horizontal chord positioned 4° below the center of the aperture (i.e., the maximal vertical extent was ∼16.5°). For stimulus presentation, a digital light processing (DLP) projector (nView) allowed us to present the stimulus in high resolution (640 × 480 pixels; 8 bits/pixel) at a rapid, noninterlaced refresh rate (∼60 Hz). The video projector operated effectively in the high intensity magnetic field of the scanning room and did not introduce any RF noise to the imaging signal.

Training Procedure

The goal of the training procedure (Phases 1 and 2) was to habituate a rhesus monkey (*Macaca mulatta*) to sit quietly in a prone position, with body restrained and head immobilized (using the aforementioned approach), in the presence of the noise of the MR imager. In Phase 1 of training, the monkey was positively reinforced for sitting in the chair while it was tilted at successively greater angles (0°, 25°, 45°, 70°, and 90°), starting at 0° and ending at 90°. The chair was tilted to each angle for five to ten successive daily sessions (∼1 hr per session) before it was tilted to the next angle. Positive reinforcement consisted of fruit and, later in the training procedure, fruit juice delivered to the monkey through a tube that was attached to a small volume pump.

When the monkey was trained to sit comfortably and quietly in the chair at a 90° angle, we began Phase 2 of the training procedure, in which she was further preconditioned for the experiment using the cylindrical primate chair and the mock fMRI environment, as described above. After the monkey habituated to this environment (∼6 weeks), the custom-designed, nonmetallic headpost was surgically attached to her skull, for head restraint. After postoperative recovery, the monkey was again trained in the simulated MR environment until she habituated to head restraint, which required ∼3 weeks. At the end of this period, the monkey was transported to the University of California San Diego MR Imaging Center for the first of two fMRI scanning sessions.

fMRI Scanning Session

For each of two sessions, the monkey was scanned in a clinical 1.5 Tesla GE SIGNA scanner with inserted local head gradient and RF coils. The monkey was placed in the magnet so that her central line of sight was parallel to the axis of the bore. The monkey viewed the visual stimulus freely (i.e., eye position was neither constrained nor monitored) by looking directly down the bore of the magnet. There was no audio associated with the visual stimulus.

There were four experiments in Session 1, and two experiments in Session 2. Each experiment consisted of eight on/off cycles, with the exception of the second experiment in Session 2, which consisted of seven on/off cycles. The stimulus (a preselected video sequence that continued across on/off cycles but was shown in the same sequence for each experiment) was presented for the duration of the "on" period (16 s, average intensity ∼20 cd/m^2). No stimulus was presented during the "off" period (16 s, ambient room lighting $<$0.5 cd/m^2). A squirt of juice (∼0.15 ml) was delivered to the monkey at the end of every other "on" cycle (i.e., every 64 s), to reinforce her for sitting quietly during the imaging experiments. In one experiment, however (fourth experiment of Session 1), juice reinforcement was delivered to the monkey at the end of every half cycle (i.e., every 16 s).

Experimental Results

In the first experiment of Session 1, we collected functional images of the posterior half of the brain (six contiguous, coronal slices, 5 mm thick). There were 202 activated voxels (2.5 × 2.5 × 5.0 mm, $r > 0.4$), and the standard deviation of the signal through time, averaged over the brain, was 5.0% of the mean brain signal. This signal variation is dominated by slight motion of the monkey through the experiment, but very strong activations were nevertheless detected in primary and extrastriate visual cortices (Figure 3). These cortical regions are well known to participate in the processing of visual input (Ungerleider and Mishkin, 1982; Macko et al., 1982; Van Essen and Maunsell, 1983). We were particularly struck by the presence of strong activation in the banks and fundus of the superior temporal gyrus (Figure 3a), which may correspond to visual areas STP (Bruce et al., 1981) and FST (Desimone and Ungerleider, 1986). By contrast, the stimulus cycles were not correlated with the fMRI time course in other, nonvisual brain regions such as the somatosensory cortex, auditory cortex, and the hippocampus (Figure 3a). The signal change was observable in each of the eight "on" periods, it exhibited the expected hemodynamic lag, and there was no evidence of artifactual correlation at the perimeter of the

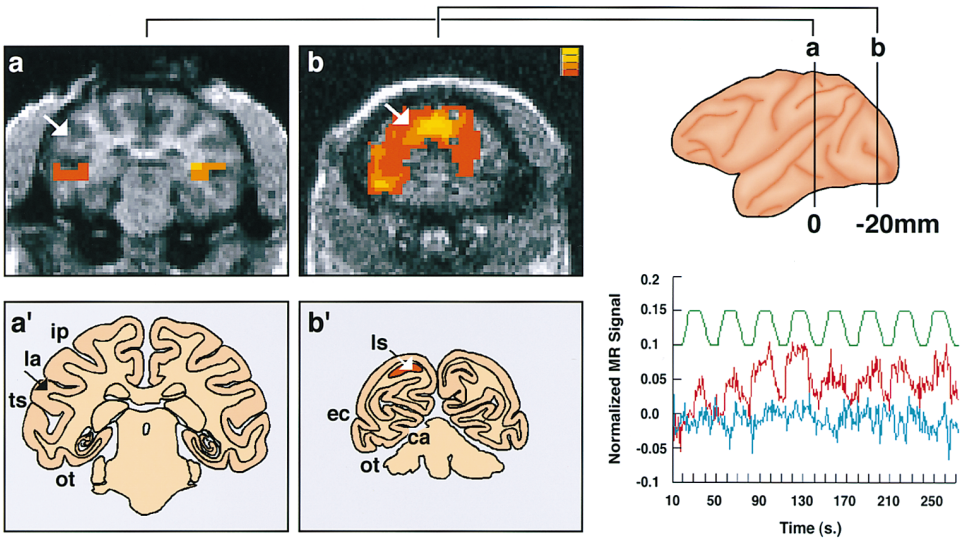

Figure 3. Images of fMRI Activation at Two Rostrocaudal Levels of the Monkey's Brain

Coronal images at two rostrocaudal levels of the monkey's brain for the first experiment of Session 1 are shown at left (a and b) along with line drawings at comparable levels (a′ and b′). The rostrocaudal location of slices is indicated in the lateral view of the brain (top right). Anatomical MR images are shown in gray scale, and areas of significant functional MR signal are overlaid in color ($r > 0.4$, $p < 10^{-9}$, uncorrected for multiple comparisons). The strongest observed changes (yellow pixels) may correspond to large veins draining activated cortex. In more moderately activated areas (orange and red pixels), signal changes were 5%–10%. (The absence of correlated pixels on the right side of the image in [b] is due to signal dropout in this area.) The activation time courses for two pixels (arrows in [a] and [b]) are illustrated in the lower right panel. An uncorrelated pixel from the superior temporal gyrus ([a], auditory cortex) is represented in blue. A highly correlated pixel from the gray matter of the lunate sulcus ([b], visual area 2 [V2]) is represented in red. The lunate sulcus is shown in red in the line drawing in (b′). The stimulus reference function is shown in green. Abbreviations: ca, calcarine sulcus; ec, external calcarine sulcus; ip, intraparietal sulcus; la, lateral sulcus; ls, lunate sulcus; ot, occipitotemporal sulcus; and ts, superior temporal sulcus.

head, which frequently occurs with stimulus-correlated motion. In this experiment, the fMRI signal contained artifacts resulting from muscle activity in the monkey's jaw and throat, which was time locked to the delivery of juice reward. By design, this artifact was uncorrelated with visual stimulation, and thus did not interfere with our ability to detect the task-related signal changes described above.

In the second and third experiments of Session 1, we collected functional images in a similar manner as the first experiment (six contiguous, coronal slices, 5 mm thick), while in the fourth experiment we collected six contiguous, sagittal slices (5 mm thick). The motion was more severe in these experiments, with gross head movements detectable in the time series, and the standard deviations of the signals were 11.0%, 10.8%, and 5.7%, respectively. This evidence for significant motion contamination was corroborated by the fact that there were also fewer voxels that passed the chosen statistical threshold for activation ($r > 0.4$) in experiments two through four (59, 66, and 29, respectively).

In Session 2, the first experiment was comparable to the first experiment of Session 1 in terms of design and collection, so we had the opportunity to directly compare the results of two experiments. Motion contamination was reduced overall in Session 2, owing to strengthening of the head-holding apparatus. Nevertheless, in the first experiment of Session 2, discrete movements were observed at the beginning and end of the time series, which were easily identified as spatially widespread, abrupt changes. The removal of those time points that were contaminated by severe motion (the first 70 and last 78 of 324 time points; e.g., Figure 4c) resulted in an improvement of the standard deviation from 2.0% to 1.3%, and produced activation maps that were similar to the maps we generated for the first experiment of Session 1 (cf. Figures 3b and 4a). There were 285 activated voxels present in the second experiment of Session 2, after we corrected for motion contamination.

For the second experiment of Session 2, we collected eight contiguous, sagittal images (5 mm thick). The standard deviation was 2.1%, and some motion was evident in the time series but was not located in discrete time blocks and was not removed. In spite of this, robust activations were detected and well localized to the posterior aspect of the brain, as expected (Figure 4b).

Discussion

These findings demonstrate that it is possible to record stimulus-induced neuronal activity-related signals in the visual cortex of an awake monkey using fMRI. Our findings are consistent with data from single-cell recording studies that have shown neuronal responses in striate and extrastriate visual areas using stimuli varied along similar dimensions (e.g., Hubel and Wiesel, 1968; Baker et al., 1981; reviewed by Maunsell and Newsome, 1987). Thus, the findings confirm the validity of these methods. It is notable, however, that similar patterns have not been seen with fMRI using anesthetized monkeys (E. DeYoe, personal communication; C. Olson, personal communication). Although it is unclear why there should be differences in the fMRI signals of alert versus

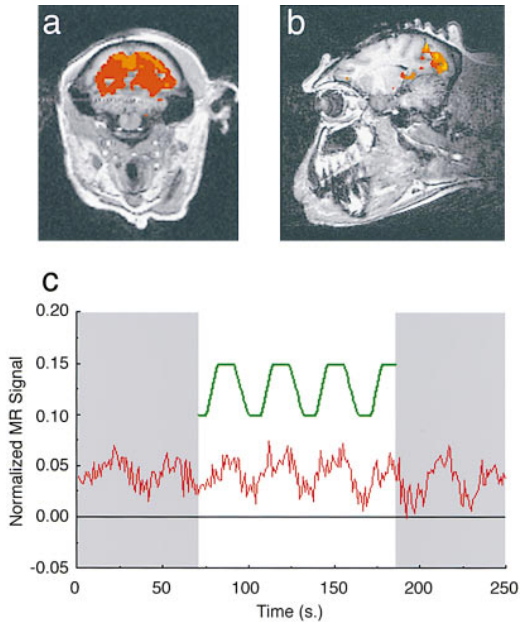

Figure 4. Images of fMRI Activation in Coronal and Parasagittal Sections through the Monkey's Brain

A coronal image of the monkey's brain for the first experiment of Session 2 (a), shown at the same rostrocaudal level as in Figure 3b. The activation time course for a pixel in the lunate sulcus (V2; see Figure 3b′) is represented in red in (c). Shading in (c) indicates the location of motion-contaminated time points that were eliminated when generating the activation map shown in (a). Also shown is a parasagittal image of the brain (b) for the second experiment of Session 2. We observed signal changes that were specific to visual cortical areas despite the presence of motion artifact in this experiment. Conventions are as in Figure 3. Activation along the edge of the brain in (a) likely did not reach statistical significance due to partial voluming effects (the voxel space sampled included brain tissue and nonbrain tissue).

anesthetized animals, the observation is consistent with the possibility that one effect of anesthesia is to decouple neuronal and vascular responsiveness (Barash et al., 1997).

While successful, there are several limitations to the procedure that we have described, and it is possible to conceive of a number of features that would make the fMRI approach in monkeys more attractive. For example, our visual stimulus presentation was limited by the fact that the accessible field of view was clipped by the magnet bore, the projected image of the stimulus extended beyond the limits of the bore, and stimulus presentation was manually controlled. A better option, which we are developing for future use, involves a binocular telescopic magnification system that will direct a much larger field of view to a distant stimulus. Stimulus presentation will also be computer driven (a routine procedure during human fMRI experiments), such that stimulus timing is more conveniently synchronized with magnet cycles.

A second area for future development involves the resolution of the fMRI signal. In the present study, 2.5 mm in-plane resolution was used because it was expected to give a signal-to-noise ratio similar to that typically achieved in human fMRI studies (3.75 mm in-plane resolution). A similar signal-to-noise ratio at this high resolution is provided by the smaller monkey RF coil. High spatial resolution, down to ~1 mm, is achievable with current scanner technology, but with a signal-to-noise ratio that is insufficient for fMRI. With custom-designed, smaller, region-specific RF coils and higher imaging fields, 1 mm resolution fMRI is foreseeable.

A third factor to be considered in optimizing the fMRI procedure in monkeys involves behavioral control during imaging sessions. In the present experiment, we neither directed nor monitored the monkey's behavior (except to confirm that she was comfortable and was indeed viewing the stimulus). The ability to constrain and monitor behavior during fMRI would significantly broaden the kinds of issues that could be addressed experimentally with this approach. Drawing further upon concepts and techniques used for single-neuron physiology in alert monkeys, it is clear that behavioral control during imaging sessions can be achieved using operant conditioning. Eye movements or manual responses, for example, can be monitored and reinforced using available technology. Regarding eye movements, we currently use a video-based eye-tracking system (ISCAN) to monitor eye movements of humans and monkeys in the laboratory, and others have used this system to monitor eye movements of humans during fMRI (Reppas et al., 1997). We are now developing techniques to bring this technology to bear on our experiments with monkey fMRI. Regarding manual responses, monkeys can easily be trained to respond using a joystick or button box (Evarts, 1966; LaMotte and Mountcastle, 1975) and should perform similarly in the MR environment. The sequence and timing of behavioral events and evaluation of the appropriateness of behavioral responses can be placed under computer control, using software designed to meet similar goals in single-neuron physiological experiments.

A potential difficulty in functional neuroimaging of awake, behaving nonhuman primates is the need to frequently reward correct experimental behavior. Consumption of the juice can have two effects that may interfere with MR signal measurement: (1) the muscle movement involved in swallowing creates magnetic field distortion that significantly changes the measured MR signal, and (2) the act of swallowing can potentially cause significant head motion, which will both disrupt signal measurement and reduce the ability to assess task-related signal changes in the entire scanning run. The movement-related effect (2) is potentially more serious but can be limited by use of a sufficiently strong device for head fixation (also see below). The magnetic field distortion (1) may be dealt with by selectively eliminating some measurements during the scanning session. Since the hemodynamic lag between evoked neural activity and the peak measurable fMRI response is generally 5 s or longer, immediate delivery of juice after a successful trial is not likely to interfere with assessment of evoked activity measured by fMRI signal change.

Finally, motion contamination was a problem for several of the experiments that we described here. Some of these motion problems may have derived from the fact that the primate chair was not anchored directly to the scanning bed within the magnet. That is, while the monkey's head may have been solidly restrained by the head-holding apparatus, her body movements may have

caused inadvertent chair movement and, because the primate chair and the head-holder are attached, consequential head movement. If this is indeed the case, the chair can easily be stabilized in future scanning sessions. While motion problems will be a central issue to address in future experiments, we have demonstrated here that, despite the presence of motion, we were nonetheless able to measure robust signal activations in an awake monkey. Importantly, because the signal change in a single experiment can be so robust, for these kinds of studies it is not necessary to average across multiple experiments to obtain statistical significance.

The use of fMRI in monkeys has a promising and exciting future. We have used the procedure described above to obtain the first evidence for activity-dependent fMRI signals in the cerebral cortex of an alert monkey. Further advances to this technique will expand the applicability of the fMRI approach to a wide range of perceptual and cognitive paradigms. Moreover, in combination with single-cell recording, fMRI in monkeys holds much promise for clarifying the neuronal events that underlie the fMRI signal. The measured fMRI signal is the end result of a long chain of physiological events, leading from changes in synaptic activity to metabolic changes to changes in cerebral blood flow, blood volume, and oxygen metabolic rate (Buxton and Frank, 1997). This physiological basis of fMRI is still poorly understood, and the information provided by combining fMRI and single-cell recording will be critical for establishing confidence in the fMRI technique as a measure of the neuronal substrates of perception and cognition in both monkeys and humans.

Experimental Procedures

Surgical Preparation and Maintenance

After an initial period of acclimation to the Phase 2 primate chair and behavioral testing apparatus, the monkey was surgically prepared for further behavioral training and fMRI signal acquisition using techniques that are used routinely for electrophysiological studies of alert monkeys (e.g., Dobkins and Albright, 1994). The surgical procedure was performed under strictly aseptic conditions using isoflurane gas (1.25% in oxygen) to invoke general anesthesia following preanesthetic drugs (Ketamine, 10 mg/kg, and acepromazine, 0.1 mg). A nonmetallic post for head restraint (Figure 2C) was affixed to extend vertically from the dorsal cranium using dental acrylic and nonmetallic screws, and the skin was drawn up around the margin of the implant. The monkey was given pre- and postsurgical prophylactic antibiotics (during surgery: 25 mg/kg Cephazolin, administered intravenously, 3 times at 2 hr intervals; after surgery: 25 mg/kg Cephazolin, administered intramuscularly at 12 hr intervals for 3 days) and postsurgical analgesics (Buprenex [buprenorphine] 0.03 mg/kg, intramuscularly, 2 times daily for 2–3 days). After healing, the cranial wound margin was treated biweekly for the duration of the experiment by removal of hair and cleansing with aseptic surgical scrub (Nolvasan) and isopropyl alcohol, followed by application of topical antibiotic, as needed.

fMRI Scanning

Functional imaging was performed in a GE 1.5 Tesla SIGNA clinical MRI scanner fitted with high performance local head gradient and RF coils (Wong et al., 1992a, 1992b, Proc. Soc. Magn. Reson. Med., abstracts). Functional T2*-weighted images were acquired using an echoplanar single-shot gradient echo pulse sequence with a matrix size of 64 $\times$ 64, echo time (TE) of 40 ms, flip angle of 90°, and in-plane resolution of 2.5 $\times$ 2.5 mm (field of view [FOV] = 16 cm). Six contiguous 5 mm coronal slices or sagittal slices were acquired in an interleaved fashion at 1 s intervals for 272 s (4 min, 32 s). In the second experiment of Session 2, eight continguous 5 mm sagittal slices were acquired for 240 s.

For anatomical localization, a whole-brain, T1-weighted three-dimensional MP-RAGE pulse sequence (written in-house) was acquired (flip angle = 10°, FOV = 16 cm, 128 $\times$ 128 $\times$ 128 acquisition matrix, sagittal slices, 1.0 mm thickness).

Prior to analysis, the first two images from each slice were discarded to assure that the MR signal had reached steady state on each slice and the images were coregistered through time using a two-dimensional registration algorithm (AFNI analysis software; Cox, 1996). Each pixel was analyzed by correlation with a reference function based on the stimulus presentation parameters with an adjustment to correct for hemodynamic lag (6 s signal rise time was assumed) and with linear drift removed.

Acknowledgments

We thank Mario Tengco and Cecelia and Jeff Manzanares for assistance in the design and construction of the primate chair, Jamie Simon for graphics assistance, and Marty Sereno for use of the nView video projector. This project was supported, in part, by a grant from the National Eye Institute (T. D. A.), by the National Institutes of Health (5 T32 MH18399 [L. S.]), and by the McDonnell-Pew Center for Cognitive Neuroscience at San Diego by the Medical Research Service of the Department of Veterans Affairs (S. Z. and L. R. S.). T. D. A. is an Investigator of the Howard Hughes Medical Institute.

Received March 9, 1998; revised May 18, 1998.

References

Baker, J.F., Petersen, S.E., Newsome, W.T., and Allman, J.M. (1981). Visual response properties of neurons in four extrastriate visual areas of the owl monkey (*Aotus trivirgatus*): a quantitative comparison of medial, dorsomedial, dorsolateral, and middle temporal areas. J. Neurophysiol. *45*, 397–416.

Barash, P.G., B.F. Cullen, and R. K. Stoelting, eds. (1997). Clinical Anesthesia, Third Edition (Philadelphia: Lippincott-Raven), pp. 705–706.

Belliveau, J.W., Kennedy, D.N., Jr., McKinstry, R.C., Buchbinder, B.R., Weisskoff, R.M., Cohen, M.S., Vevea, J.M., Brady, T.J., and Rosen, B.R. (1991). Functional mapping of the human visual cortex by magnetic resonance imaging. *254*, 716–719.

Bruce, C., Desimone, R., and Gross, C.G. (1981). Visual properties of neurons in a polysensory area in superior temporal sulcus of the macaque. J. Neurophysiol. *46*, 369–384.

Buxton, R.B., and Frank, L.R. (1997). A model for the coupling between cerebral blood flow and oxygen metabolism during neural stimulation. J. Cereb. Blood Flow Metab. *17*, 64–72.

Courtney, S.M., and Ungerleider, L.G. (1997). What fMRI has taught us about human vision. Curr. Opin. Neurobiol. *7*, 554–561.

Cox, R.W. (1996). AFNI: software for analysis and visualization of functional magnetic resonance neuroimages. Comput. Biomed. Res. *29*, 162–173.

Desimone, R., and Ungerleider, L.G. (1986). Multiple visual areas in the caudal superior temporal sulcus of the macaque. J. Comp. Neurol. *248*, 164–189.

Dobkins, K., and Albright, T.D. (1994). What happens if it changes color when it moves? The nature of chromatic input to macaque visual area MT. J. Neurosci. *14*, 4854–4870.

Evarts, E.V. (1966). Pyramidal tract activity associated with a conditioned hand movement in the monkey. J. Neurophysiol. *29*, 1011–1027.

Hubel, D.H., and Wiesel, T.N. (1968). Receptive fields and functional architecture of monkey striate cortex. J. Physiol. (Lond.) *195*, 215–243.

LaMotte, R.H., and Mountcastle, V.B. (1975). Capacities of humans and monkeys to discriminate vibratory stimuli of different frequency

and amplitude: a correlation between neural events and psychological measurements. J. Neurophysiol. *38*, 539–559.

Macko, K.A., Jarvis, C.D., Kennedy, C., Miyaoka, M., Shinohara, M., Sokoloff, L., and Mishkin, M. (1982). Mapping the primate visual system with [2–^{14}C] deoxyglucose. Science *281*, 394–397.

Maunsell, J.H.R., and Newsome, W. (1987). Visual processing in monkey extrastriate cortex. Annu. Rev. Neurosci. *10*, 363–401.

Raichle, M.E. (1998). Behind the scenes of functional brain imaging: a historical and physiological perspective. Proc. Natl. Acad. Sci. USA *95*, 765–772.

Reppas, J.B., Niyogi, S., Dale, A.M., Sereno, M.I., and Tootell, R.B. (1997). Representation of motion boundaries in retinotopic human visual cortical areas. Nature *388*, 175–179.

Ungerleider, L.G., and Mishkin, M. (1982). Two cortical visual systems. In Analysis of Visual Behavior, D.J. Ingle, M.A. Goodale, and R.J.W. Mansfield, eds. (Cambridge, MA: MIT Press), pp. 549–598.

Van Essen, D.C., and Maunsell, J.H.R. (1983). Hierarchical organization and functional streams in the visual cortex. Trends Neurosci. *9*, 370–375.